Collective Motion

- Nuclear Vibrations
- Nuclear Rotations
- Collective degrees of freedom differ from single-particle effects
- Require proper description (new models)

Experimental signatures

- E(2+)
- B(E2; 2+ –> 0+)

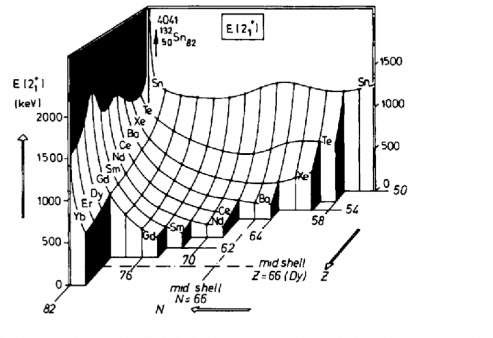

Figure 12.1. Landscape plot of the energy of the first excited 2^+ state $E_x(2_1^+)$ in the region $50 \leq Z \leq 82$ and $50 \leq N \leq 82$. The lines connect the $E_x(2_1^+)$ values in isotope chains (taken from Wood 1992).

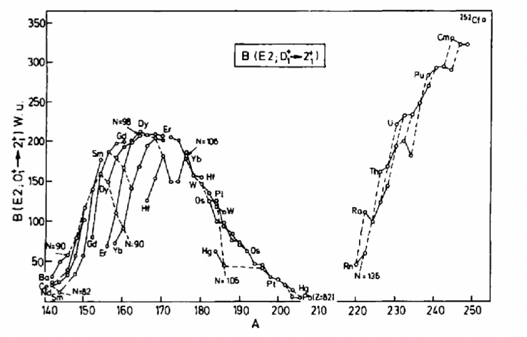

Figure 12.2. Systematics of the $B(E2; 0_1^+ \rightarrow 2_1^+)$ values for the even–even nuclei with $N \geq 82$, $Z \leq 98$. The $B(E2)$ values are expressed in Weisskopf units (WU) (taken from Wood 1992).

Nuclear vibrations

- Major mode for nuclear vibrations (quantised!) is the quadrupole vibration
- Can be described as fluctuations on the nuclear density distribution around a spherical (or even deformed) equilibrium shape
- One can start from the liquid-drop model and build a coherent description of nuclear vibrations

Nuclear vibrations

$$R(\theta, \varphi) = R_0\left(1 + \sum_{\lambda\mu} \alpha_{\lambda\mu} Y^*_{\lambda\mu}(\theta, \varphi)\right).$$

R is the radius in the direction (θ,φ) of the nuclear surface

λ describes the multipolarity of the shape

Dynamics:

$$H_{\text{vibr}} = \sum_{\lambda,\mu} \frac{B_\lambda}{2} |\dot{\alpha}_{\lambda\mu}|^2 + \sum_{\lambda,\mu} \frac{C_\lambda}{2} |\alpha_{\lambda\mu}|^2.$$

Vibrational modes

momentum $\pi_{\lambda,\mu} = B_\lambda \dot{\alpha}^*_{\lambda\mu}$ or $-i\hbar\partial/\partial\dot{\alpha}_{\lambda\mu}$

$$b^+_{\lambda\mu} = \sqrt{\frac{\omega_\lambda B_\lambda}{2\hbar}}\left(\alpha_{\lambda\mu} - \frac{i}{\omega_\lambda B_\lambda}(-1)^\mu \pi_{\lambda-\mu}\right)$$
$$b_{\lambda\mu} = \sqrt{\frac{\omega_\lambda B_\lambda}{2\hbar}}\left((-1)^\mu \alpha_{\lambda-\mu} + \frac{i}{\omega_\lambda B_\lambda}\pi_{\lambda\mu}\right). \qquad (12.5)$$

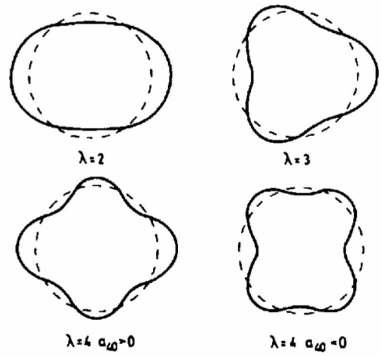

Figure 12.4. Nuclear shape changes corresponding to quadrupole ($\lambda = 2$), octupole ($\lambda = 3$) and hexadecupole ($\lambda = 4$) deformations (taken from Ring and Schuck 1980).

Nuclear vibrations

$$[b_{\lambda'\mu'}, b^+_{\lambda\mu}] = \delta_{\lambda\lambda'}\delta_{\mu\mu'}$$

$$\omega_\lambda = \sqrt{C_\lambda/B_\lambda}.$$

$$H_{vibr} = \sum_\lambda \hbar\omega_\lambda \sum_\mu (b^+_{\lambda\mu} b_{\lambda\mu} + \tfrac{1}{2})$$

A multiphonon (normalized) state

$$\prod_{\lambda\mu} \frac{(b^+_{\lambda\mu})^{n_{\lambda\mu}}}{\sqrt{n_{\lambda\mu}!}}|0\rangle.$$

$$J = 0,\ 2,\ 4$$

$$|n_2 = 2; JM\rangle = \frac{1}{\sqrt{2}} \sum_{\mu_1\ \mu_2} \langle 2\mu_1, 2\mu_2 \mid JM\rangle b^+_{2\mu_1} b^+_{2\mu_2}|0\rangle$$

Multi-phonon quadrupoles states

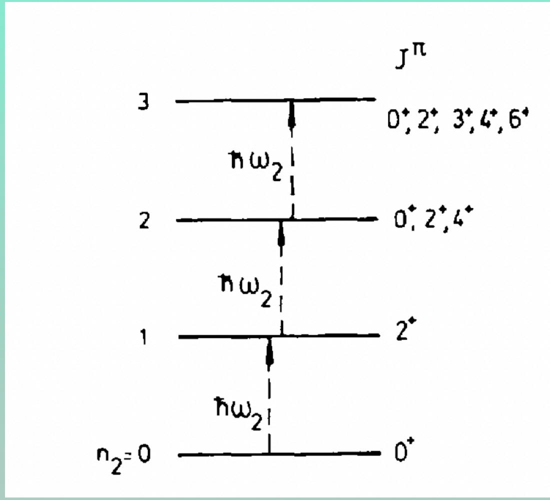

λ-pole transition operator

$$\mathcal{M}(E\lambda, \mu) = \frac{Ze}{A} \int d^3 r\, r^\lambda Y'_{\lambda\mu}(\hat{r}) \rho(\vec{r}).$$

In expanding the density around the equilibrium value ρ_0 but always using a constant density for $r \leq R_0$ and vanishing density outside ($r > R_0$), we obtain

$$\rho(\vec{r}) \cong \rho_0(r) - R_0 \frac{\partial \rho_0}{\partial r} \sum_{\lambda\mu} \alpha_{\lambda\mu} Y^*_{\lambda\mu}(\hat{r}) + \theta(\alpha^2)$$

$$\mathcal{M}(E\lambda, \mu) = \frac{3}{4\pi} Ze R_0^\lambda \left(\frac{\hbar}{2\omega_\lambda B_\lambda} \right)^{1/2} (b^+_{\lambda\mu} + (-1)^\mu b_{\lambda, -\mu})$$

B(Eλ)

So, the $E\lambda$ radiation follows the selection rule $\Delta n_\lambda = \pm 1$ and the $E\lambda$ moments of all states vanish. The $B(E\lambda; \lambda \to 0^+)$ for the $n_\lambda = 1 \to n_\lambda = 0$ transition becomes

$$B(E\lambda; \lambda \to 0^+) = \left(\frac{3R_0^\lambda Ze}{4\pi}\right)^2 \frac{\hbar}{2\omega_\lambda B_\lambda}, \qquad (12.13)$$

and one obtains the ratio in $B(E2)$ values for the quadrupole vibrational nucleus

$$B(E2; 4_1^+ \to 2_1^+) = 2B(E2; 2_1^+ \to 0_1^+). \qquad (12.14)$$

Typical values for the $B(E2; 2_1^+ \to 0_1^+)$ values are of the order of 10–50 Weisskopf units (wu). A number of these ratios are fully independent of the precise values of the C_λ, B_λ coefficients and are from a purely geometric origin.

Vibrational modes

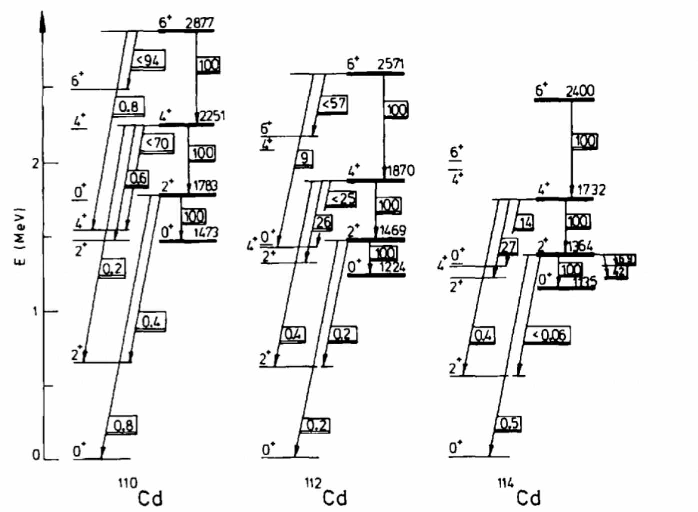

Figure 12.6. Relative $B(E2)$ values for the deformed bands in ^{110,112,114}Cd (thick lines). The other excitations present part of the multi-phonon quadrupole vibrational spectrum (taken from Wood *et al* 1992).

compare with HO

equidistant phonon energies are observed

Best examples in the Cd, Pd region

examples of vibrational nuclei

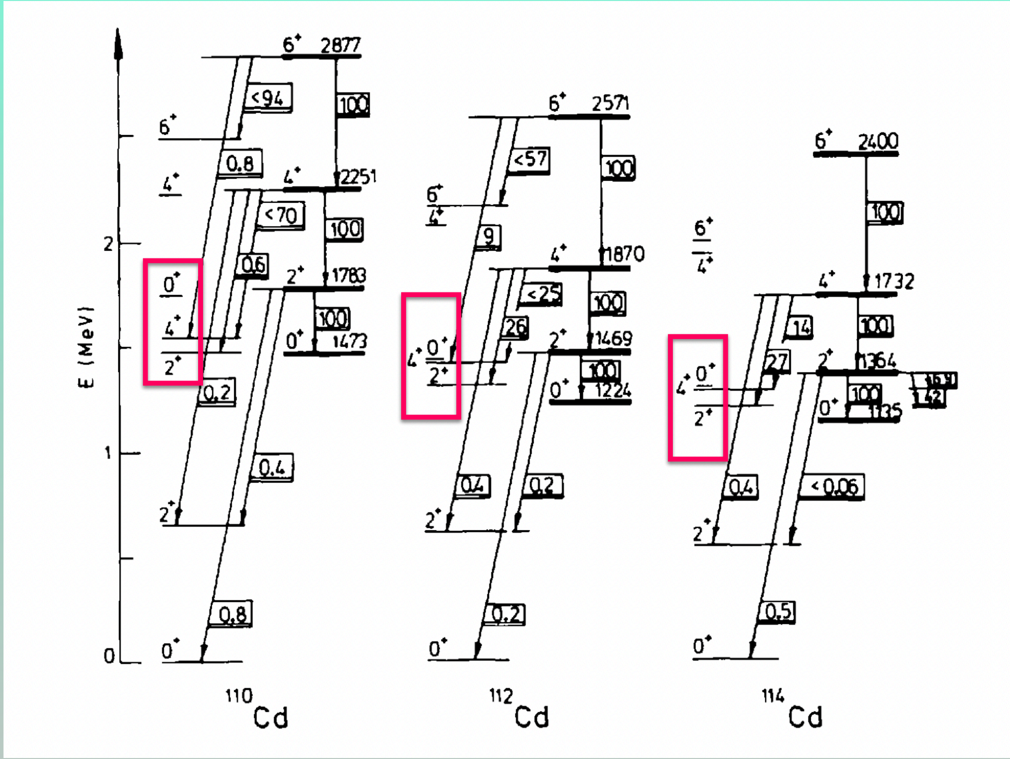

examples of vibrational nuclei

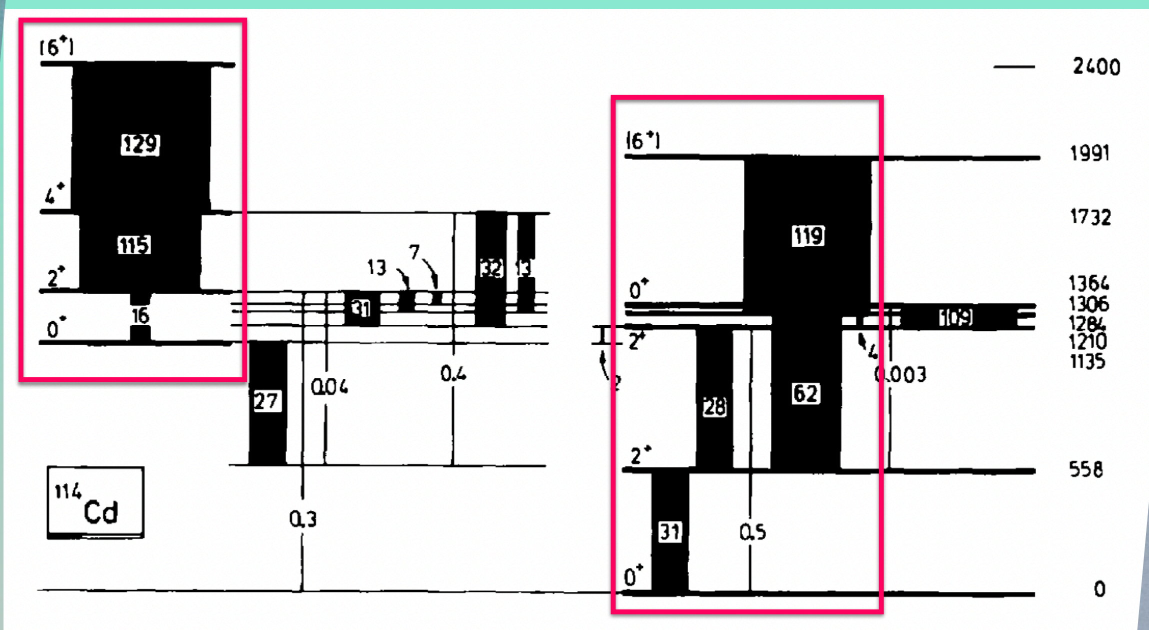

examples of vibrational nuclei

$$B_\lambda = \frac{1}{\lambda}\frac{3AmR_0^2}{4\pi},$$

with m the nucleon mass and $R_0 = r_0 A^{1/3}$

$$C_\lambda = (\lambda-1)(\lambda+2)R_0^2 a_s - \frac{3(\lambda-1)}{2\pi(2\lambda+1)}\frac{Z^2e^2}{R_0}$$

a_s = 18.56 keV

Do deviations exist?
Is the vibrational model successful?

Systematics

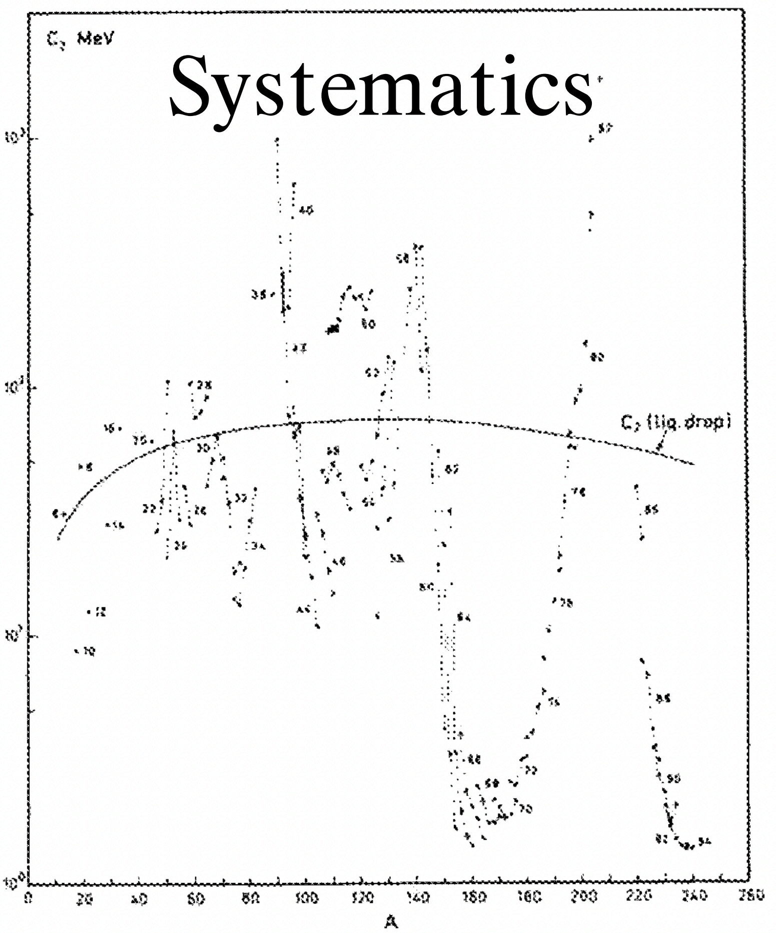

Sum rules

$$S(E\lambda) = \sum_f (E_f - E_0) B(E\lambda; 0 \to \lambda_f).$$

$$S(E\lambda) = \frac{1}{2} \sum_\mu \langle 0 | [[\mathcal{M}(E\lambda, \mu), H], \mathcal{M}^*(E\lambda, \mu)] | 0 \rangle.$$

$$\mathcal{M}(E\lambda, \mu) = e \sum_p r_p^\lambda Y_{\lambda\mu}(\hat{r}_p).$$

$$[\mathcal{M}(E\lambda, \mu), H] = \frac{\hbar^2}{m} e \sum \vec{\nabla}(r^\lambda Y_{\lambda\mu}(\hat{r})) \cdot \vec{\nabla}$$

$$[[\mathcal{M}(E\lambda, \mu), H], \mathcal{M}^*(E\lambda, \mu)] = \frac{\hbar^2}{m} e^2 \sum \vec{\nabla}(r^\lambda Y_{\lambda\mu}(\hat{r})) \cdot \vec{\nabla}(r^\lambda Y^*_{\lambda\mu}(\hat{r}))$$

Sum rules

$$S(E\lambda) = \frac{Ze^2\hbar^2}{2m} \sum_\mu \langle 0 | \vec{\nabla}(r^\lambda Y_{\lambda\mu}(\hat{r})) \cdot \vec{\nabla}(r^\lambda Y^*_{\lambda\mu}(\hat{r})) | 0 \rangle$$

$$= \frac{Ze^2\hbar^2}{2m} \frac{\lambda(2\lambda+1)^2}{4\pi} \langle r^{2\lambda-2} \rangle.$$

for constant density, incl. isospin:

$$S(E\lambda)_{T=0} = \frac{3}{4\pi} \lambda(2\lambda+1) \frac{Z^2 e^2 \hbar^2}{2mA} R_0^{2\lambda-2}$$

typically, a low-lying collective state is ~10% of the T=0 sum rule

Nuclear rotations

- Nuclear rotations are
- The Bohr Hamiltonian is involved for rotational nuclei
- Spherical nucleic can not exhibit rotational features
- Axial shapes are ideal for such studies

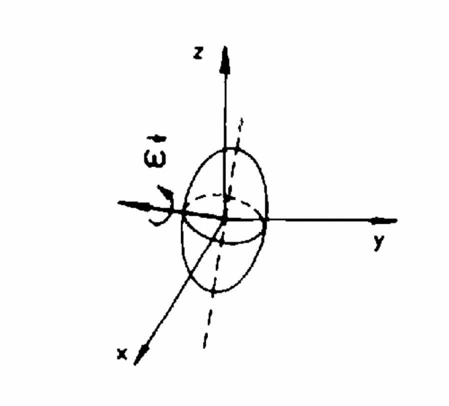

Nuclear rotations

transformed collective variables $a_{\lambda\mu}$ to the laboratory $\alpha_{\lambda\mu}$ values.

$$Y_{\lambda\mu}(\text{rotated}) = \sum_{\mu'} D^{\lambda}_{\mu'\mu}(\Omega) Y_{\lambda\mu'}(\text{lab})$$

$$a_{\lambda\mu} = \sum_{\mu'} D^{\lambda}_{\mu'\mu}(\Omega) \alpha_{\lambda\mu'}.$$

the nuclear radius $R(\theta, \varphi)$ remains invariant under a rotation

Using the transformation from the lab into the rotated, body-fixed axis system, the five $\alpha_{2\mu}$ reduce to *two* real independent variables a_{20} and $a_{22} = a_{2-2}$ (with $a_{21} = a_{2-1} = 0$).

$$a_{20} = \beta \cos\gamma$$

$$a_{22} = \frac{1}{\sqrt{2}} \beta \sin\gamma$$

Nuclear rotations

$$R(\theta,\varphi) = R_0\left\{1+\beta\sqrt{\frac{5}{16\pi}}(\cos\gamma(3\cos^2\theta-1)+\sqrt{3}\sin\gamma\sin^2\theta\cos 2\varphi)\right\}$$

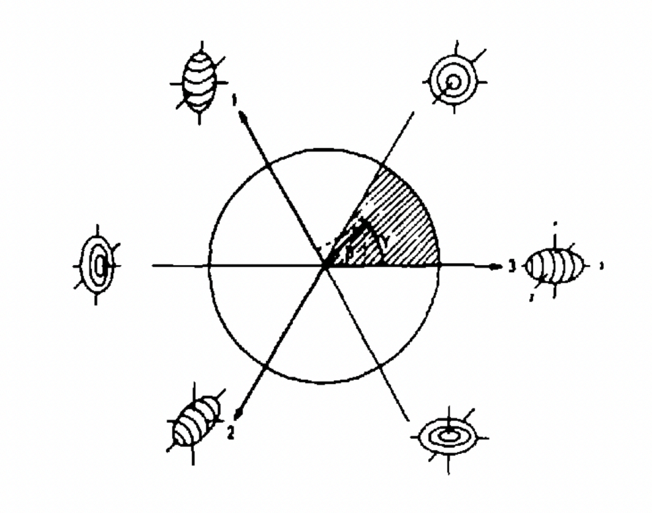

Nuclear rotations

(a) γ values of 0°, 120° and 240° yield prolate spheroids with the 3, 1 and 2 axes as symmetry axes;

(b) γ = 180°, 300° and 60° give oblate shapes;

(c) with γ not a multiple of 60°, triaxial shapes result;

(d) the interval $0° \leq \gamma \leq 60°$ is sufficient to describe all possible quadrupole deformed shapes;

(e) the increments along the three semi-axes in the body-fixed systems are evaluated as

$$\delta R_1 = R\left(\frac{\pi}{2},0\right) - R_0 = R_0\sqrt{\frac{5}{4\pi}}\beta\cos\left(\gamma-\frac{2\pi}{3}\right)$$

$$\delta R_2 = R\left(\frac{\pi}{2},\frac{\pi}{2}\right) - R_0 = R_0\sqrt{\frac{5}{4\pi}}\beta\cos\left(\gamma+\frac{2\pi}{3}\right)$$

$$\delta R_3 = R(0,0) - R_0 = R_0\sqrt{\frac{5}{4\pi}}\beta\cos\gamma. \qquad (12.32)$$

$$\delta R_k = R_0\sqrt{\frac{5}{4\pi}}\beta\cos\left(\gamma-\frac{2\pi}{3}k\right) \qquad k = 1,2,3.$$

Collective potential surfaces

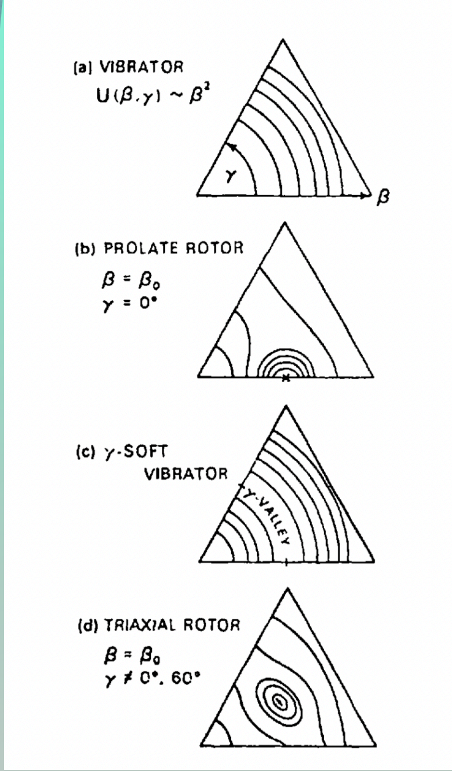

Bohr Hamiltonian becomes

$$H = T(\beta, \gamma) + U(\beta, \gamma),$$

$$U(\beta, \gamma) = \tfrac{1}{2}C_{20}(a_{20}(\beta, \gamma) - a_{20}^{-})^2 + C_{22}(a_{22}(\beta, \gamma) - a_{22})^2$$

$$T = T_{\mathrm{rot}} + \tfrac{1}{2}B_2(\dot{\beta}^2 + \beta^2\dot{\gamma}^2)$$

$$T_{\mathrm{rot}} = \frac{1}{2}\sum_{k=1}^{3}\mathcal{J}_k\omega_k^2.$$

$$\mathcal{J}_k = 4B_2\beta^2\sin^2\left(\gamma - \frac{2\pi}{3}k\right) \qquad k = 1, 2, 3.$$

Bohr Hamiltonian

For fixed values of β and γ, T_{rot} is the collective rotational kinetic energy with moments of inertia $\mathcal{J}_k$. With β, γ changing, the collective rotational and β, γ vibrational energy become coupled in a complicated way. Using the irrotational value for B_2 (section 12.1), these irrotational moments of inertia become

$$\mathcal{J}_k^{\mathrm{irrot}} = \frac{3}{2\pi}mAR_0^2\beta^2\sin^2\left(\gamma - \frac{2\pi}{3}k\right) \qquad k = 1, 2, 3, \qquad (12.39)$$

whereas for *rigid* body inertial moments, one derives

$$\mathcal{J}_k^{\mathrm{rigid}} = \frac{2}{5}mAR_0^2\left(1 - \sqrt{\frac{5}{4\pi}}\beta\cos\left(\gamma - \frac{2\pi}{3}k\right)\right) \qquad k = 1, 2, 3. \qquad (12.40)$$

Bohr Hamiltonian

We can remark that: (i) $\mathcal{J}^{\text{irrot}}$ vanishes around the symmetry axes; (ii) $\mathcal{J}^{\text{irrot}}$ shows a stronger β-dependence ($\sim \beta^2$) compared to a β-dependence only in $\mathcal{J}^{\text{rigid}}$; (iii) the experimental moments of inertia $\mathcal{J}^{\text{exp}}$ can, in a first step be derived from the 2_1^+ excitation energy assuming a pure rotational $J(J+1)$ spin dependence. A relation with the deformation variable β can be obtained with the result

$$\mathcal{J}^{\text{exp}} \simeq \frac{\hbar^2 \beta^2 A^{7/3}}{400} (\text{MeV}^{-1}). \qquad (12.41)$$

$$\mathcal{J}^{\text{irrot}} < \mathcal{J}^{\text{exp}} < \mathcal{J}^{\text{rigid}}$$

Systematics

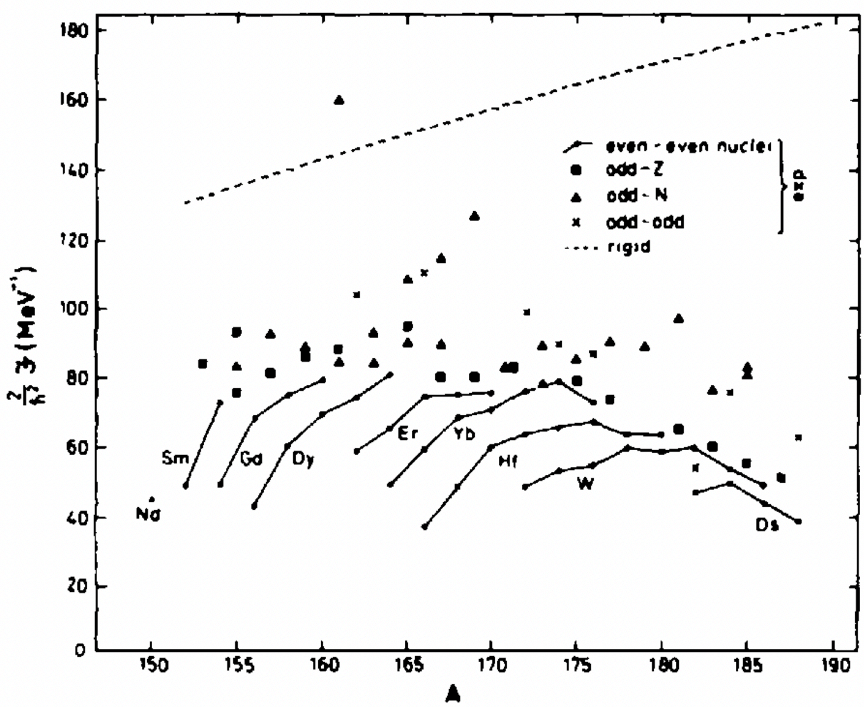

Bohr Hamiltonian

$$\hat{H}_{\text{coll}} = \frac{-\hbar^2}{2B_2}\left[\beta^{-4}\frac{\partial}{\partial\beta}\left(\beta^4\frac{\partial}{\partial\beta}\right) + \frac{1}{\beta^2\sin 3\gamma}\frac{\partial}{\partial\gamma}\left(\sin 3\gamma\frac{\partial}{\partial\gamma}\right)\right] + \hat{T}_{\text{rot}} + U(\beta,\gamma), \quad (12.43)$$

with

$$\hat{T}_{\text{rot}} = \frac{\hat{I}_1^2}{2\mathcal{J}_1} + \frac{\hat{I}_2^2}{2\mathcal{J}_2} + \frac{\hat{I}_3^2}{2\mathcal{J}_3}. \quad (12.44)$$

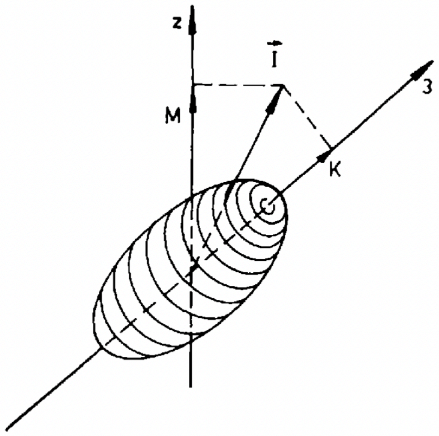

Rotational W-F

for the collective wavefunction is

$$|\psi_M^J\rangle = \sum_K g_K(\beta,\gamma)|JMK\rangle,$$

$$|JMK\rangle = \sqrt{\frac{2J+1}{8\pi^2}}\,D_{MK}^J(\Omega).$$

K=0

(i) $K = 0$ *bands* ($J_3 = 0$). The wavefunction, since rotational axial vibrational motions decouple, now becomes

$$|\psi^J_{M,K=0}\rangle = g_0(\beta, \gamma)|J, M, K = 0\rangle. \qquad (12.48)$$

A spin sequence $J = 0, 2, 4, 6, \ldots$ appears and describes the collective, rotational motion. For the vibrational motion, one can approximately also decouple the a_{20} (β-vibrations) from the a_{22} (γ-vibrations) oscillations. Superimposed on each vibrational (n_β, n_γ) state, a rotational band is constructed, according to the energy eigenvalue

$$E_{n_\beta, n_\gamma}(J) = \hbar\omega_\beta(n_\beta + \tfrac{1}{2}) + \hbar\omega_\gamma(2n_\gamma + 1) + \frac{\hbar^2}{2\mathcal{J}_0}J(J+1), \qquad (12.49)$$

with $n_\beta = 0, 1, 2, \ldots$; $n_\gamma = 0, 1, 2, \ldots$ and with ω_β and ω_γ the β and γ vibrational frequencies.

K≠0

Here, symmetrized, rotational wavefunctions are needed to give good parity, with the form

$$|\psi^J_{M,K}\rangle = g_K(\beta, \gamma)\frac{1}{\sqrt{2}}[|JMK\rangle + (-1)^J|JM-K\rangle], \qquad (12.50)$$

and with even K values. For such $K \neq 0$ bands, the spin sequence results with $J = |K|$, $|K|+1$, $|K|+2, \ldots$. Here now, the γ-vibration couples to the rotational motion, with the resulting energy spectrum

$$E_{K,n_\beta,n_\gamma}(J) = \hbar\omega_\beta(\eta_\beta + \tfrac{1}{2}) + \hbar\omega_\gamma\left(2n_\gamma + 1 + \frac{|K|}{2}\right) + \frac{\hbar^2}{2\mathcal{J}_0}[J(J+1) - K^2]. \quad (12.51)$$

Realistic cases

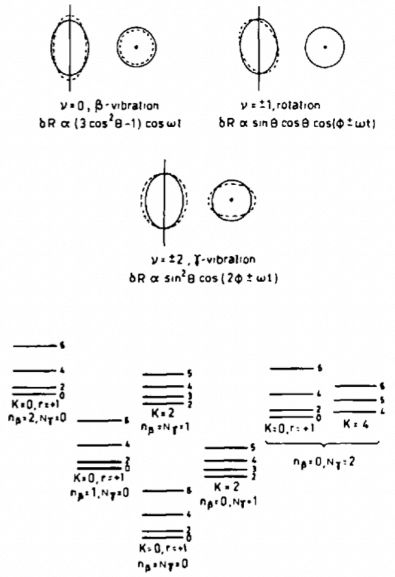

Figure 12.18. Various quadrupole shape oscillations in a spheroidal nucleus. The upper part shows projections of the nuclear shape in directions perpendicular and parallel to the symmetry axis. The lower part shows the spectra associated with excitations of one or two quanta, including the specific values of the various oscillation energies $\hbar\omega_\beta$, $\hbar\omega_\gamma$. The value of N_γ used in the figure that classifies the gamma vibration is defined as $N_\gamma = 2n_\gamma + |K|/2$. The rotational energy is assumed to be given by $J(J+1) - K^2$ and harmonic oscillatory spectra are considered. (Taken from Bohr and

Realistic cases

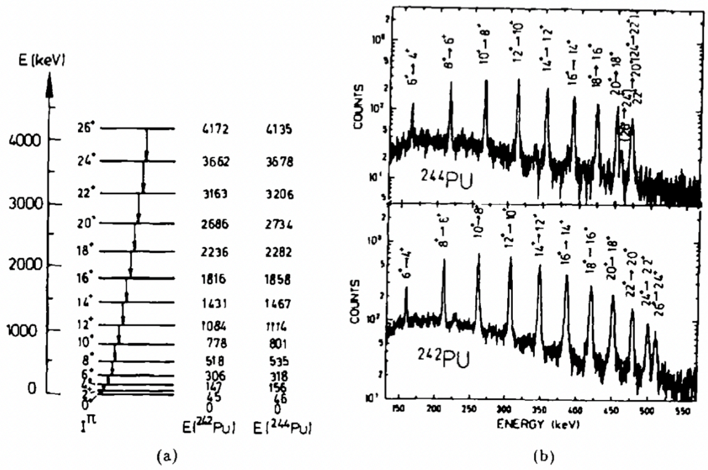

Figure 12.19. (*a*) Band structure observed in ^{242,244}Pu. The $E2$ transitions connecting the members of the band are shown by arrows. The gamma lines corresponding to these transitions are marked, e.g., $6^+ \rightarrow 4^+$ (at ~ 160 keV) in part (*b*). The discontinuity in transition energy at high spin is discussed in Chapter 13. (*b*) Coulomb excitation with 5.6–5.8 MeV/u ^{208}Pu. Doppler shift-corrected gamma spectra for ^{242}Pu and ^{244}Pu are shown (Spreng *et al* 1983) (taken from Wood 1992).